Fluvial response to sudden input of pyroclastic sediments during the 2008–2009 eruption of the Chaitén Volcano (Chile): The role of logjams

Aldo M. Umazano [a, b, *], Ricardo N. Melchor [a, b], Emilio Bedatou [a, b], Eduardo S. Bellosi [c], Javier M. Krause [d]

[a] INCITAP (Consejo Nacional de Investigaciones Científicas y Técnicas – Universidad Nacional de La Pampa), Avenida Uruguay 151, 6300 Santa Rosa, La Pampa, Argentina
[b] Facultad de Ciencias Exactas y Naturales, Universidad Nacional de La Pampa, Avenida Uruguay 151, 6300 Santa Rosa, La Pampa, Argentina
[c] Consejo Nacional de Investigaciones Científicas y Técnicas – Museo Argentino de Ciencias Naturales, Avenida Ángel Gallardo 470, 1405 Buenos Aires, Argentina
[d] Consejo Nacional de Investigaciones Científicas y Técnicas – Museo Paleontológico Egidio Feruglio, Avenida Fontana 140, U9100GYO Trelew, Chubut, Argentina

ARTICLE INFO

ABSTRACT

The rhyolitic Plinian eruption of the Chilean Chaitén Volcano, initiated on May 2, 2008, suddenly introduced abundant pyroclastic sediments in the Blanco River catchment area, which experienced important modifications. Before May 2, the river was characterised by gravelly and moderate to low-sinuosity channels crossing a vegetated and locally urbanised (Chaitén City) floodplain. This river, limited by steep and densely forested highlands, was connected with the Pacific Ocean via a tidally-influenced delta plain. After heavy rains in May 11–20, the river discharge increased and triggered several responses including logjam formation and breakage, crevassing, avulsion (and channel abandonment), changes in the pattern and dimensions of channels, and construction of a new delta plain area. In this context, the goals of this contribution were: i) to document the sedimentological processes within a detailed geomorphic framework and ii) to understand the influence of logjams on fluvial dynamics. Upstream of the logjam zone, the deposits are mostly composed of ash and lapilli with abundant palaeovolcanic (epiclastic) sediments, which were produced by dilute currents and debris flows. Downstream of the logjam zone, deposits are composed by ash and lapilli, both pumice-rich and lacking important participation of older (epiclastic) sediments. The abandoned and filled palaeochannel, and the proximal part of crevasse splays experienced transient dilute flows with variable sediment concentration and, subordinately, hyperconcentrated flows. The distal sectors of crevasse splays mostly record settling from suspension. At the delta plain, tephra transported by the Blanco River was mixed with older sediments by tide and wave action (dilute flows). We conclude that immediately after eruption, both geomorphic and sedimentary processes of the river were mainly controlled by a combination of high availability of incoherent pyroclastic sediments on steep slopes, abundant rains, large logs that jammed the river and huge areas of devastated forest. Logjams played an important role in the river response to the volcanic eruption; they were responsible of the marked compositional change recorded upstream and downstream of the logjam zone and its breakage resulted in downstream flooding and avulsion. The likelihood of formation of logjams in rivers draining forested volcanic areas should be considered in the evaluation of volcanic hazards related to Plinian eruptions.

1. Introduction

The input of large volume of pyroclastic sediments in fluvial environments causes different types of disturbances in the landscape and, in many cases, triggers processes that constitute relevant risks for humans, their activities and constructions. These sediments derive from: i) the volcanic edifices via ash-falls, surges or

* Corresponding author. Facultad de Ciencias Exactas y Naturales, Universidad Nacional de La Pampa, Avenida Uruguay 151, 6300 Santa Rosa, La Pampa, Argentina. Tel.: +54 02954 245220x7318.
E-mail addresses: amumazano@exactas.unlpam.edu.ar, amumazano@yahoo.com.ar (A.M. Umazano), rmelchor@exactas.unlpam.edu.ar (R.N. Melchor), ebedatou@yahoo.com (E. Bedatou), ebellosi@sei.com.ar (E.S. Bellosi), mkrause@mef.org.ar (J.M. Krause).

hot pyroclastic flows and ii) the remobilisation of primary or reworked pyroclastic deposits. Independently of their origin, tephra influx induces important hydrological modifications linked to the sudden and high sediment supply (e.g. Montgomery et al., 1999; Major et al., 2000; Major, 2003; Major and Yamakoshi, 2005; Major and Mark, 2006). The hydrological changes include several aspects such as decrease in soil infiltration, both waxing and waning runoff, and increase of transport capacity and generation of peak flows. Moreover, the fluvial systems experience complex geomorphic adjustments and changes in the processes of transport and sedimentation. The first adjustments comprise modifications in size and patterns of channel belts, which frequently cause intricate histories of avulsions and reoccupations (e.g. Major, 2003; Gran and Montgomery, 2005; Kataoka et al., 2008; Gran et al., 2011; Kataoka, 2011). Coevally, the high pyroclastic influx coupled with high slopes and water availability induces the generation of flows with high concentration of sediments covering the debris flow-hyperconcentrated flow continuum (lahars *sensu* Smith and Lowe, 1991). The lahars are conspicuous features of most fluvial environments affected by explosive volcanism (e.g. Naranjo et al., 1986; Cronin et al., 1997; Gran and Montgomery, 2005; Manville et al., 2009a; Graettinger et al., 2010). These can be triggered in a number of ways including rainfall, melting of snow or ice, breaching of lakes and channel damming (Smith and Lowe, 1991). Other landscape disturbances include biological aspects such as reduction or elimination of plant cover (Vessell and Davies, 1981).

Particularly, the literature on detailed descriptions of both modern and recent fluvial systems affected by rhyolitic volcanism is scarce. It includes examples from the area surrounding the 1991 eruption of Mount Pinatubo from the Philippines (e.g. Gran et al., 2011; Gran and Montgomery, 2005), the 1.8 ka Taupo eruption in New Zealand (e.g. Manville et al., 2005, 2009b,c) and some Japanese Plio-Pleistocene tephras (Kataoka and Nakajo, 2002). These contributions have documented the geomorphic evolution and associated sedimentary processes, as well as their intra- and inter-basinal controlling factors. These controlling factors are commonly temporal changes in the rate of introduced volcaniclastic material, proximity to the eruptive centre, and distribution of pyroclastic flow deposits, which can generate transient jams in the rivers.

In this context, the rhyolitic explosive eruption of the Chilean Chaitén Volcano, which initiated on May 2008 and introduced pyroclastic sediments in the rivers draining the Michinmahuida−Chaitén highlands, offers an excellent opportunity for increasing the knowledge about the interaction between a fluvial system and acidic Plinian volcanism. In particular the Blanco River catchment, located adjacent to the Chaitén Volcano, was heavily loaded with pyroclastic material (Lara, 2009; Alfano et al., 2011; Romero, 2011; Pierson et al., 2013) and experienced important geomorphic and sedimentological responses mainly related to generation and rupture of logjams (Umazano et al., 2013). Consequently, the goals of the paper are: i) to document the sedimentological processes triggered by the Chaitén 2008−2009 eruption in the Blanco River drainage basin within a detailed geomorphic framework and ii) to understand the influence of logjams on fluvial dynamics, and possible consequences for volcanic hazards evaluation.

2. Study area: geology and physiography

The Chaitén Volcano (43° 83′ S; 72° 65′ W) is located in southern Chile, towards the W−SW of the larger Michinmahuida Volcano (Fig. 1) and associated to the Liquiñe Ofqui fault zone (Hervé, 1976). It is one among more than 120 active continental volcanoes of the Chilean Andes (Lara, 2009). Before the 2008 eruption, the Chaitén Volcano was a 3 km in diameter nearly circular caldera with a

height of 940 m above middle sea level. At least two previous volcanic events are recorded for this volcano. The older originated a 3−4 km diameter caldera at about 9.4 ka, which was probably accompanied by both rhyolitic pumice-rich pyroclastic flows and ash falls (Naranjo and Stern, 2004). Later, the caldera was partially filled by an obsidian dome; the age of this event is estimated at 5.6 ka using archeological data (Alfano et al., 2011). Recently, the occurrence of younger eruptive deposits has been suggested (Watt et al., 2013), including one of circa 300 years (Lara et al., 2013).

Near the Chaitén Volcano, there are three main rivers that drain water and sediments from the Andes towards the Pacific Ocean (Fig. 1). One of these, the Blanco or Chaitén River, begins about 9 km to the SE of the volcano, and runs adjacent to its southern slope. From there, several gullies feed the river, which flows approximately for 7 km more from the foot of the volcano to its mouth in the Pacific Ocean. The Chaitén City, the unique town affected by eruption-related floods, is placed close to its mouth. The Blanco River catchment area (77 km^2) supports a dense temperate rain forest; recent annual rainfall (2004−2009) in the region surrounding Chaitén Volcano ranged from about 2500 mm to 7000 mm (Pierson et al., 2013).

This study was carried out in the medial−distal part of the Blanco River, from 2 km downstream of the southern slope of the volcano to the Pacific Ocean (Fig. 1). The area studied in detail is nearly rectangular and covers approximately 15 km^2.

3. History of the 2008−2009 eruption

Chaitén Volcano suddenly erupted on May 2, 2008, without important previous indicators. The Liquiñe Ofqui fault zone was active prior to the Chaitén event, triggering other volcanic explosions (e.g. in the Cordón Caulle and Villarrica Volcanoes; Romero, 2011), as well as seismic activity in the Aysén fjord (Romero, 2011). Less than two days before the first explosion, a short seismic swarm up to 5° magnitude was recorded in a 20 km radius area from the volcano (Lara, 2009), as the only precursor activity. According to Castro and Dingwell (2009), volcanic activity started with some ash emissions on May 1, but the first large explosion began on May 2, at 08:00 h (UT), when Chaitén Volcano experienced a Plinian eruption caused by rapid ascent of rhyolitic magma (Castro and Dingwell, 2009; Major and Lara, 2013). The explosion formed a 21 km high eruptive column followed by lava dome building and ash plumes (Lara, 2009; Major and Lara, 2013). On the next day, and after a short period of calm, a new explosion formed a 17−20 km high column (Durant et al., 2012). After the second explosion seismicity decreased greatly but ash emission continued until May 6, when at 12:32 h (UT) a third Plinian column reached a 30 km elevation (Carn et al., 2009; Lara, 2009; Durant et al., 2012). The last large Plinian explosion was on May 8, at 03:36 h (UT), forming a 20−22 km high pyroclastic column (Carn et al., 2009; Durant et al., 2012). These columns partially collapsed, producing small pyroclastic flows mostly within the caldera and, in few cases, in the eastern and northern flanks of the volcano (Lara, 2009; Major and Lara, 2013). The later travelled up to 2−3 km from the crater (Romero, 2011) severely damaging the forest. All pyroclastic flows related to these explosions were topographically controlled (Lara, 2009; Romero, 2011). Few days after the start of the eruption, on May 10−12, the extrusion of a new dome began (Carn et al., 2009). Dome growing was accompanied by ash and steam emission, which continued by several months with small random increments in column height (Lara, 2009). During dome growing several collapses occurred inside the caldera (Romero, 2011), as well as in the proximity of the volcano along the Blanco River valley (Major et al., 2013).
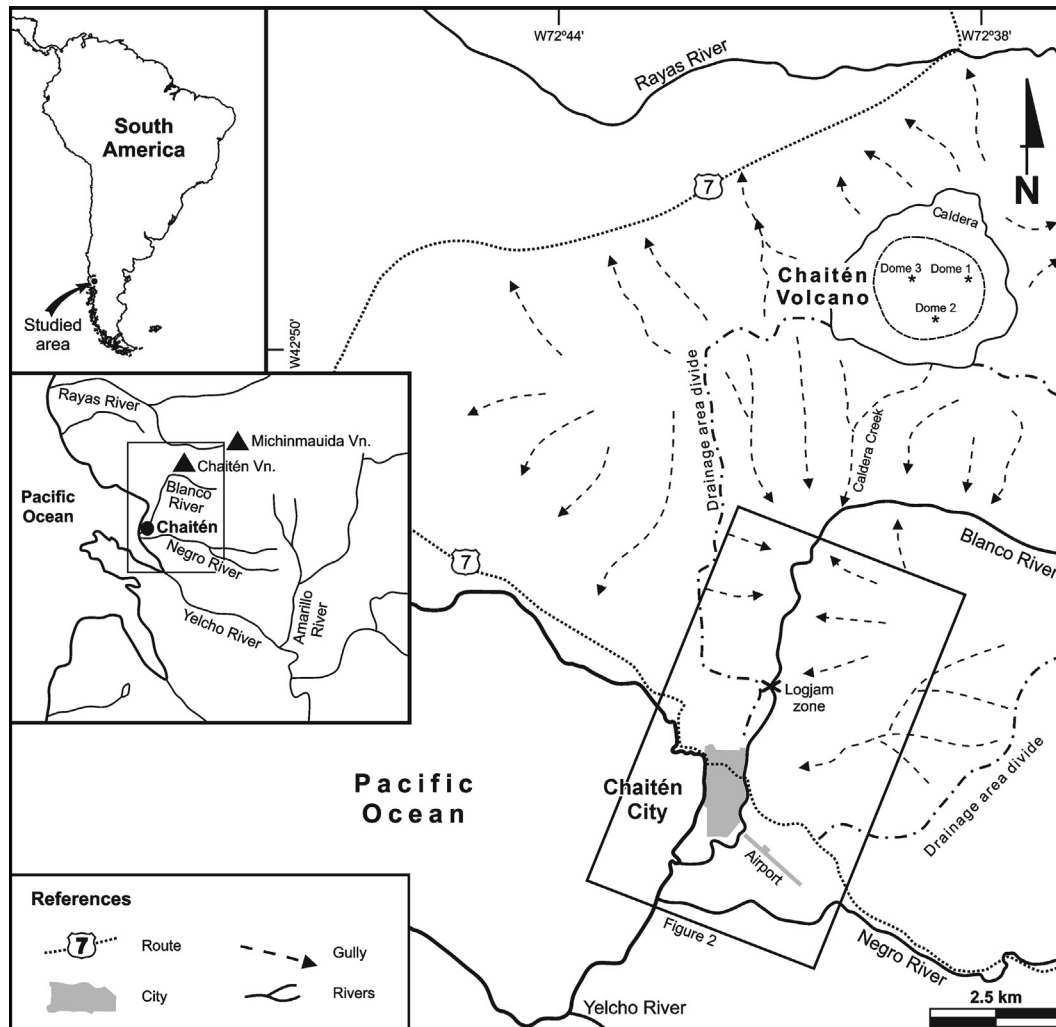
Fig. 1. Location map of the Chaitén volcano and the study area. The shoreline adjacent to Chaitén City and Blanco River course is drawn after its configuration prior to May 2008.

A new dome building phase was initiated on February 9, 2009. This dome collapsed on February 19, resulting in a lateral blast and pyroclastic flows (Carn et al., 2009; Romero, 2011), which travelled throughout the Blanco River valley approximately 10 km downstream of the volcano (Major et al., 2013). Later, between April and September of that year, a third dome grew in the amphitheatre product of the previous collapse (Romero, 2011). Until mid 2013, the volcano was active although stable according to information published by SERNAGEOMIN the Servicio Nacional de Geología y Minería de Chile (http://www.sernageomin.cl/volcanes.php).

Using theoretical models of eruption column height, the volume of extruded material during Plinian eruptions (2–8 May) was from 1 to 4 km³ (non Dense-Rock Equivalent) of magma (Lara, 2009); but other researchers estimated volumes not higher than 1 km³ based on deposited ash (Watt et al., 2009; Alfano et al., 2011). Prevailing wind patterns of southern South America (Prohaska, 1976; Paruelo et al., 1998) favoured dispersion of ash plumes toward the east and southeast of the volcano, settling most of it in Argentina and in the Atlantic Ocean (Carn et al., 2009; Watt et al., 2009; Alfano et al., 2011; Durant et al., 2012).

4. Methodology

Pre- and syn-eruptive geomorphology of the study area was mapped using satellite images (Google Earth™) and aerial photos published in several papers and in reports by SERNAGEOMIN. During the field work (November–December 2009, February 2011 and December 2012), the syn-eruptive geomorphical units were checked and refined. The thickness of the 2008–2009 eruption flood deposits was measured in natural cuts, open pits or estimated employing a screw auger. At selected sites, open pits were excavated using hand shovel and logged in detail. Seventeen representative detailed sedimentary logs were chosen for this study. The presence of a shallow water table was a complicating factor to obtain complete sections (i.e., reaching the pre-eruptive substrate) because the lower part of several open pits commonly collapsed within a few minutes after excavation. The attributes observed during logging were lithology, grain size, sorting, grading and sedimentary structures. Common measured current indicators were long axes of oriented logs. The terms volcaniclastic gravel (VG) and volcaniclastic sand (VS) were used for secondary pyroclastic sediments with appreciable mixing with epiclastic sediments. The adjective reworked was employed to characterise those remobilised pyroclastic sediments lacking significant mixing with epiclastic detritus: reworked lapilli (RL) and reworked ash (RA). In addition, the latter was subdivided in coarse-grained (sand-sized, RCA) and fine-grained (mud-sized, RFA). Sedimentary facies were defined following the proposal by Miall (1978): capital and small letters to indicate the lithology and sedimentary structure, respectively. Shapes of sediment bodies were classified according to width, length and thickness (Bridge, 1993).

5. Geomorphic evolution

Before May 2, 2008, the Blanco River was characterised by a low to moderate sinuosity fluvial channel-belt that, in N–S orientation, crossed a heavily vegetated and locally urbanised (Chaitén City) floodplain (Fig. 2A). Valley side and head slopes average 35°–45° (ridge to valley), with some slope segments reaching up to 70° (Pierson et al., 2013). This pre-eruptive fluvial system can be divided into two sectors with different geomorphic features: upstream and downstream of the Blanco River bridge, denominated
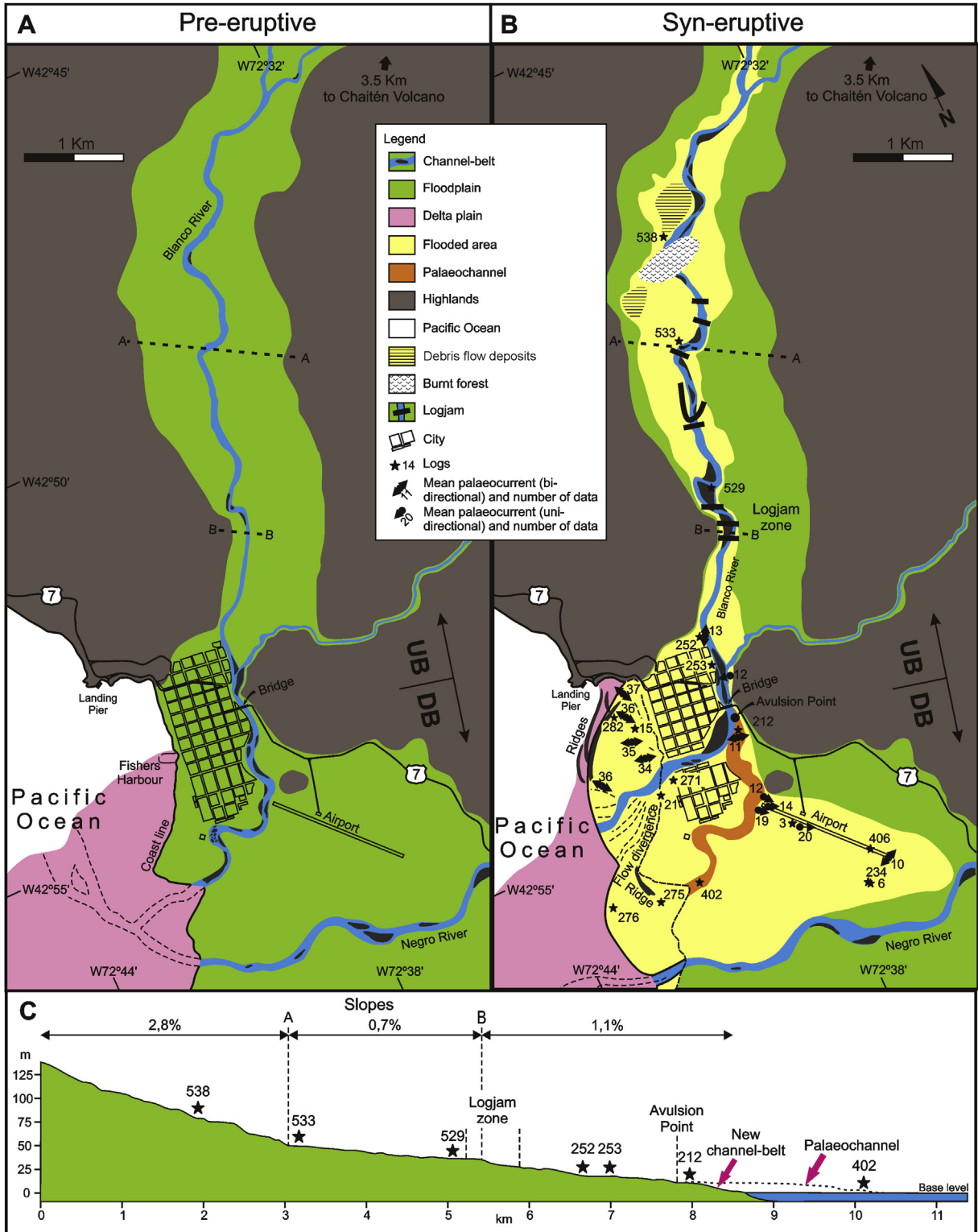

Fig. 2. Geomorphic evolution of the study area. (A) Pre-eruptive scenario. (B) Syn-eruptive scenario. Note location of detailed sedimentary logs and palaeocurrent data measured from long axes of oriented logs. (C) Topographic profile along the Blanco River reflecting pre- and syn-eruptive features.

herein as UB and DB respectively (Fig. 2A). The UB sector showed a 60 m–200 m wide channel belt with low sinuosity (1.23) and, locally, a few bars attached to their margins (straight-like channel pattern) (Table 1). The adjacent floodplain, limited by steep highlands, ranged in width from 500 m to 3000 m. Just upstream of the bridge, there were two margin-related bars at the confluence with a tributary on the left margin. The DB sector had a moderate sinuosity (1.51) fluvial channel belt with common presence of attached-margin bars and, less frequently, longitudinal bars (meandering-like channel pattern, Table 1). The distal part of this 40 m–130 m wide channel-belt crossed a complex tide and wave-influenced delta plain and emptied in the Pacific Ocean. In this DB sector of the fluvial system, the floodplain on the right margin of the channel-belt, where most of the Chaitén City is located, was 700 m–900 m wide. The floodplain on the left margin of the channel-belt was probably affected by floods from the adjacent Negro River and, consequently, its width is uncertain. The topographic gradient along the channel-belt diminishes towards the sea; it is 2.8% upstream of point A, from there to point B (coincident with the future logjam zone) the value is 0.7% and, downstream of point B it reaches 1.1% (Fig. 2C). Both upstream and downstream of the Blanco River bridge, clast-supported gravels overlain by pedogenised deposits are exposed underlying the 2008–2009 reworked tephra, thus suggesting that former river transport was by dilute tractive processes (Fig. 3). These gravelly deposits are similar to those found in the bed of the active channel about one and a half year after the eruption, when the pyroclastic sediment load decreased significantly.

On May 11, 2008 the Blanco River increased its water level by more than 1.5 m (Alfano et al., 2011; Romero, 2011), a phenomenon linked to breakout of logjams (see next section). This caused the crevassing at both margins of the river (Fig. 2B) and, consequently, the flooding of the Chaitén City, which was evacuated six days before (Lara, 2009). Initially, the flood ponded within a few blocks at the western side of the channel-belt but, as the flooding continued, on May 20, about 98% of the Chaitén City houses were damaged (Romero, 2011). In addition, the landscape experienced other important and drastic modifications including changes in the fluvial style (Figs. 2B and 4A), avulsion (Figs. 2B and 4B), crevassing (Figs. 2B and 4C,D) and enlargement of the subaerial delta plain (Figs. 2B and 4E). In this syn-eruptive scenario, the UB sector is characterised by a wider (60–440 m) and low sinuosity (1.28) channel-belt with braided and margin-related bars (braided-like style) (Table 1). The channel-belt of DB sector changed its position just downstream of the bridge (avulsion point in Fig. 2B). Analysis of aerial photos suggests that this process occurred prior to May 15 and ended by May 20 (Pierson et al., 2013). In the DB track, the previous NNE–SSW strike of the stream was changed to ENE–WSW direction, forming an angle of approximately 33°. Before avulsion, the channel-belt widened (up to about 210 m wide) without relevant changes in its sinuosity. The distal part of the now abandoned channel-belt has lobe geometry and contains abundant and large transported logs mostly aligned in the previous direction of the flow. At present, this palaeochannel is fully filled with reworked tephra from the 2008–2009 eruption and partially covered by aeolian dunes nucleated on shrubby vegetation (Fig. 4B). The new and active channel-belt, which is placed in the location of a former street of the city (Fig. 4A), shows low sinuosity (1.13) and braid bars and rarer margin-related bars immediately downstream of the avulsion point (braided-like channel patter, Table 1). The lower reach of the current channel of the Blanco River has been stabilised by continuous rock embankments to protect the city from flooding (Fig. 4A) and its width ranges from 50 m to 100 m. At present, the topographic gradient along the fluvial course is roughly similar to those described for the pre-eruptive condition; the main difference is a larger slope downstream of the avulsion point (about 8.8%) probably due to post May 2008 incision (Fig. 2C). This new fluvial course added a portion of subaerial delta plain that coalesces with that produced by the Negro River progradation (Figs. 2B and 4E).

6. Deposits and sedimentary processes

The thickness of the primary pyroclastic fall deposits reach more than 0.20 m near the Chaitén Volcano and diminish in a southeast direction towards the Atlantic coast of Argentina (Watt et al., 2009; Melchor et al., 2010; Alfano et al., 2011). The maximum ash fall thickness in areas that were not flooded is about 20 mm. These deposits will be treated in a future contribution, along with the modern biogenic structures produced in them. The reworked deposits related to the eruption, in some places mixed with older sediments, can reach several metres in the study area, particularly in the channel-margins upstream of the bridge and within the filled palaeochannel. Commonly, these deposits overlie a buried soil developed on ancient volcaniclastic strata or an artificial pavement in the flooded portion of the city and airport. Composition of detritus transported in the syn-eruptive stage is variable along the fluvial course. Upstream of the logjam zone the deposits are composed of ash and lapilli with abundant palaeovolcanic sediments with low to nule vesicularity (effusive rock fragments), whereas downstream of the logjam zone the deposits are constituted of ash and lapilli, both pumice-rich and without important participation of epiclastic sediments.

In this section, we will first treat the logjams found in the Blanco River (Figs. 5 and 6) and then describe and interpret the syn-eruptive sedimentary record of selected geomorphic sectors (Figs. 7–12). They are denominated as follow: i) channel-margin upstream of the logjam zone, ii) filled palaeochannel, iii) right crevasse splay, iv) left crevasse splay and v) delta plain (Fig. 2B). The description and interpretation of the different sedimentary facies is summarised in Table 2; Figs. 13 and 14 contain illustrations of the main recognised sedimentary facies. Palaeocurrent data from oriented logs is plotted in Fig. 2B.

Table 1
Synopsis of the main geomorphic features of the Blanco River during pre and syn-eruptive periods distinguishing between the upstream bridge (UB) and downstream bridge (DB) sectors.

	Pre-eruptive		Syn-eruptive	
	UB	DB	UB	DB
Channel-belt width	60–200 m	40–130 m	60–440 m	50–100 m[a]
Sinuosity	1.23	1.51	1.28	1.13
Bar types	Few, margin attached	margin attached and longitudinal bars	Braid bars and very scarce margin attached	Braid bars and very scarce margin attached
Channel pattern	Straight-like	Meandering-like	Braided-like	Braided-like

[a] This track was controlled by rock embankments.

Fig. 3. Buried soil with *in situ* tree stumps developed on pre-eruptive gravels overlain by syn-eruptive volcaniclastic sediments. Person in the background (arrowed) is 1.75 m high.

6.1. Logjams

Description. The formation of jams composed of large logs and gravel was an essential aspect of the Blanco River sedimentary dynamics during the May 2008 flood (e.g., Iroume et al., 2010; Umazano et al., 2013). Logjams were recognised in the area upstream of the Blanco River bridge (UB track), and were particularly abundant in a zone located about 2.2 km upstream of the bridge. This zone is here named the logjam zone and contains, at least, three large logjams in less than 0.5 km of river valley (Figs. 2B and 5A,B,D). The logjam zone corresponded with a sharp curve of the river channel with margin attached bars prior to the eruption, and is now a zone of increased sinuosity (about 1.9; Fig. 6A and B). The Blanco River gradient well upstream of the logjam zone is 2.8% and decreases markedly just before the logjam zone to 0.7%. Downstream of the logjam zone the average gradient is 1.1%. In addition to this difference in gradient, the location of the logjam zone is aligned with the nearby mountain front (Fig. 2B). At least five additional large logjams were identified in a linear distance of 2.5 km along the river valley upstream of the logjam zone (Fig. 2B). A particular case of logjam is arcuate in plan view and thus includes not only the damming of the channel but also its margins,
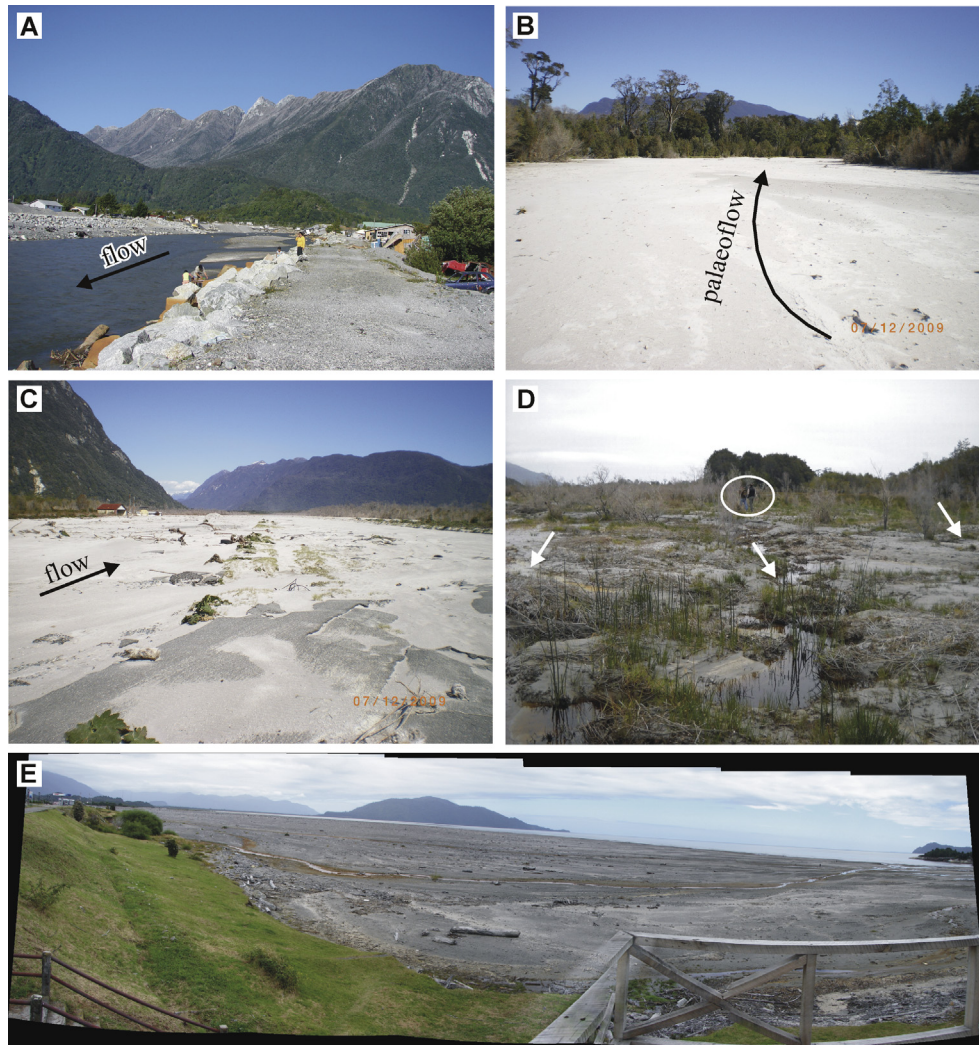
Fig. 4. Photos of different geomorphic sectors of the study area. (A) Present course of the Blanco River downstream of the avulsion point (looking upstream). Note rock embankment and in-channel bars. Person for scale. (B) Filled palaeochannel looking downstream. (C) Proximal left crevasse splay along the airstrip looking southeast (downstream). Note remains of the pavement of airstrip in the foreground. (D) Distal portion of the left crevasse splay at the wetland; note the presence of low-relief floodplain channels (arrowed). Persons in the background (circled) for scale. (E) Delta plain constructed by progradation of the Blanco River into the Pacific Ocean. View to the west from Chaitén City.

Fig. 5. Views of logjams. (A) Remains of a logjam (arrowed) from the logjam zone, formed against standing trees. River flow is toward right. (B) Two logjams (arrows) from the logjam zone, looking upstream. (C) Remains of a minor logjam (arrow), left margin, downstream of logjam zone. (D) Detail of the front of a logjam looking upstream. Note logs of different size stranded against standing trees (now dead) and the trapping of sediments. (E) Arcuate logjam formed on the channel and its right margin, looking downstream. Note the May 2008 terrace (black arrow) and r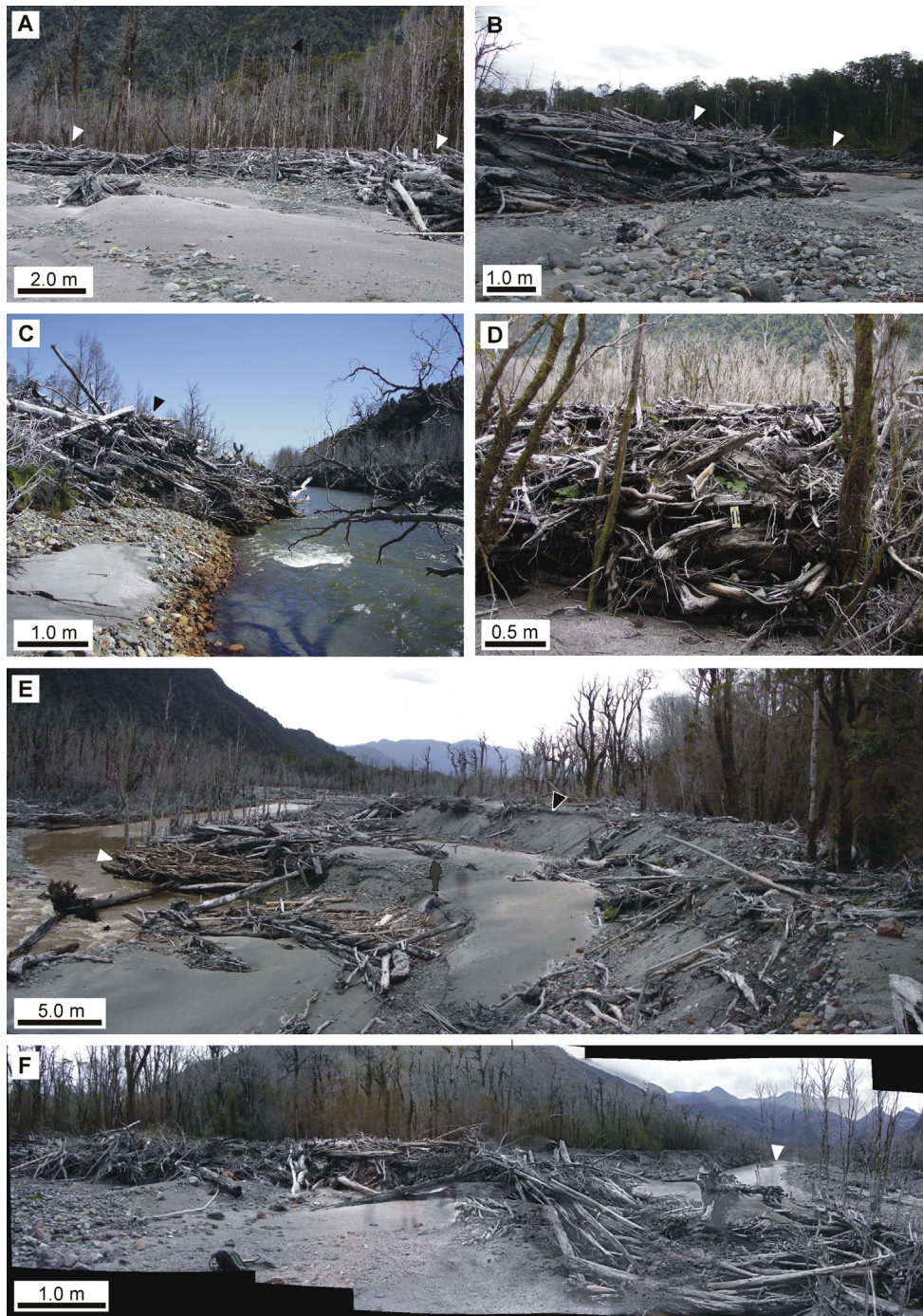emains of large logs that formed the nucleus of the jam (white arrow). See also Fig. 6B and C. (F) Panoramic view of the downstream portion of the arcuate logjam taken from the May 2008 terrace. Note current position of Blanco River (arrow). All pictures were taken on December 2012, except for C (February 2011).

especially on the right margin (Figs. 2B, 5E,F and 6B,C). At the downstream end this logjam is about 6 m high and the lateral dam height decreases upstream to level with the surrounding floodplain in about 0.35 km (Fig. 5E). At the downstream end this logjam is about 6 m high at the channel position and the height difference with the surrounding floodplain is about 2 m (Figs. 5D and 6C). Logs composing the jams can be up to 1 m in diameter and more than 10 m long.

Interpretation. The drainage basin of the Blanco River contains a hygrophilous forest with trees that may reach more than 1 m in diameter and several tens of meters high. During the pre-eruptive period, the near-channel area was heavily forested (Fig. 5A). Log-jams were produced where floodwaters transporting logs found standing trees near the channel. Logs were stranded against upright trees with the largest axis perpendicular to the current along with large blocks or pebbles (Fig. 5C and D). In this way, river discharge
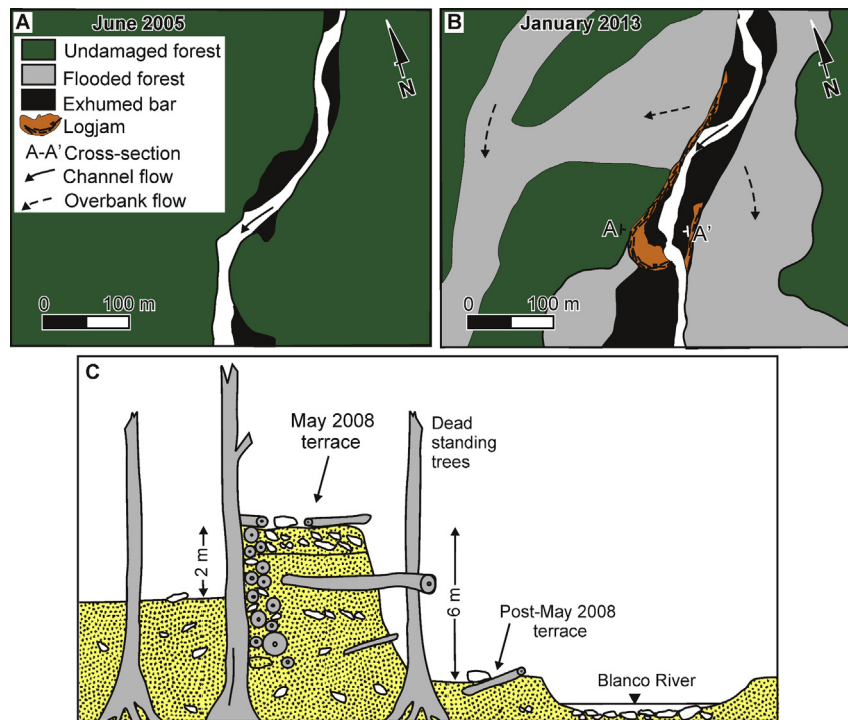
Fig. 6. Diagram of the arcuate logjam. (A) and (B) Pre- and syn-eruptive scenario (2005 and 2013) for the track of the river where the arcuate logjam was formed. Note the presence of a sharp curve and reduction of channel width. Diagrams constructed using Google Earth® images. (C) Schematic cross-section of the arcuate logjam, showing the May 2008 terrace (showing a similar composition that those of section 533, Fig. 8), the flooded floodplain (left) and current position of the river.

was reduced or prevented by obstruction of channels, and sediment and water was trapped in the dam. Devastated forest due to volcanic blasts, burning and subsequent mass wasting phenomena related to heavy rains, in addition to dead wood material lying in the forest, sourced the logjams. Logjam breakage produced a sudden release of water, sediments and logs feeding further overbank flows in the downstream area (crevasse-splays), and triggered channel avulsion. The location of the logjam zone along the mountain front can be interpreted as reflecting a control by faulting.

6.2. Channel-margin upstream of the logjam zone

Description. In this zone, thickness of the deposits diminishes downstream, from approximately 10 m in the northern part of the study area to less than 1 m in the logjam zone (Figs. 7 and 8). An overall wedge shape is inferred for the 2008–2009 eruption deposits in both margins of the channel-belt. In this part of the fluvial system, three measured sedimentary logs were selected (logs 538, 533 and 529 in Fig. 8; see their locations in Fig. 2B). All sections are characterised by a lower part composed of reworked coarse-grained ash, and an upper part constituted by an alternation of volcaniclastic gravels and volcaniclastic coarse to fine-grained sands. The ash usually shows trough cross-bedding (facies RCAt) and, less commonly, plane-parallel lamination (facies RCAh) or massive aspect (facies RCAm) (Fig. 13D and E). Around standing trees, centroclinal cross stratification (Underwood and Lambert, 1974) was identified (Fig. 13F). The upper part of the log 538, located in the most upstream position and near of the confluence with a tributary, is dominated by massive and matrix-supported volcaniclastic gravels (facies VGmm) with clasts up to 2.2 m long (Fig. 14B). Presence of uncharred logs and upright tree stumps is common (Fig. 3). This facies is interbedded with imbricated, crudely stratified gravels (facies VGh, Fig. 14A and C) associated with minor amounts of sandy and gravelly beds with trough cross-bedding (facies VSt and VGt, respectively). The upper part of sections 533

and 529 typically displays stratified gravels with clast imbrication (facies VGh) and trough cross-bedded sands (facies VSt) (Fig. 14C). Subordinately, the sands exhibit plane-parallel lamination (facies VSh) or are massive (facies VSm) (Fig. 14A), and the gravels have trough cross-bedding (facies VGt). Although not logged in detail, another occurrence of the massive volcaniclastic gravel facies was identified on the right side of the valley between sections 538 and 533 (Fig. 2B). These 4.5 m thick deposits are associated with a minor tributary and its maximum clast size is 0.15 m.

Interpretation. The lower part of the three sections records the reworking of pyroclastic substrates by dilute flows with different sediment concentration (Smith and Lowe, 1991). These sediments are considered the typical May 2008 flood deposits. Facies RCAm indicates type 2 dilute flows, which are turbulent but with a high sediment concentration that precludes bedform generation and, therefore, produces massive beds. Facies RCAt and RCAh suggest type 1 dilute flows (common streamflow in which the different bed configurations can be developed) with migration of sinuous-crested (3D) dunes and plane beds, respectively. Centroclinal cross-strata are typical of flow disturbance by standing trees and are the result of flooding of a forested floodplain. Facies VGmm, which is dominant in the upper part of the log 538, is compatible with debris flows (deposition by in masse freezing); the intercalations of facies VGh represent temporal reduction in sediment concentration and reworking of previous deposits by dilute and high energy stream-flow (Cronin et al., 1999). The remaining facies of these logs were generated by dilute flows with low sediment/water ratio (Smith and Lowe, 1991), which formed three dimensional dunes (facies VGt and VSt) and plane beds (facies VSh), as well as more concentrated flows in the more downstream log (facies VSm).

6.3. Filled palaeochannel

Description. The actual cross-section geometry of this channel-belt succession, which was active probably until May 15–20,
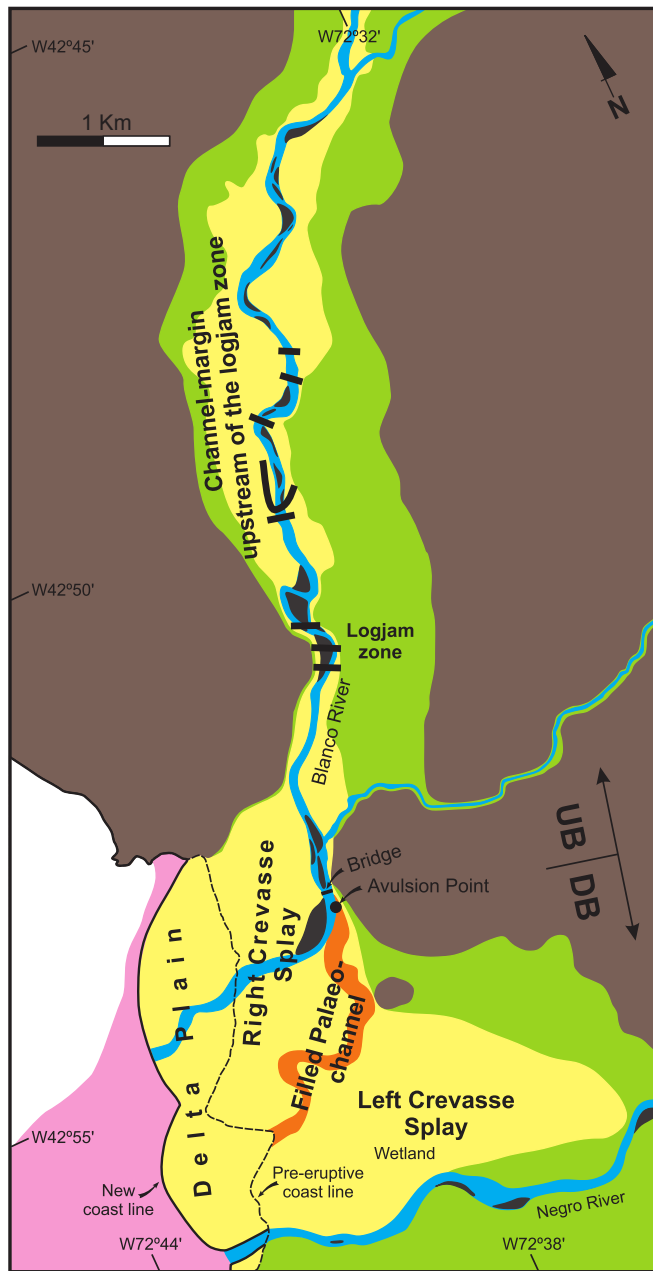
Fig. 7. Location of described geomorphic sectors in the syn-eruptive scenario. Note the change in the coastline and progradation of a new delta lobe after eruption-related river flooding.

2008, remains obscure because the pre-eruptive substrate was not reached and exposed in most sites. Nevertheless, a channel-like form is inferred from a partial cross-section view (Fig. 15) and from the thickness of the measured sections. In a section parallel to channel axis the strata exhibit a sheet-like geometry. The interfluve between the abandoned palaeochannel of the Blanco River and the Negro River contain a thin (0.07–0.25 m thick) bed of fine-grained ash lying on the pre-2008 soil (Fig. 2B). Two sedimentary logs were measured to describe the palaeochannel succession (logs 212 and 402 in Figs. 2B and 9). Log 212, placed immediately downstream of the avulsion point, has 2.6 m of minimum thickness and includes reworked coarse-grained ash interbedded with reworked lapilli. Lapilli beds typically have scoured bottoms, are massive in the base and pass-upward to plane parallel lamination (facies RLm and RLh, respectively). In other cases, the lapilli beds show trough cross-

bedding (facies RLt) or crude stratification with inversely-graded pumice fragments (facies RLs) (Fig. 13B). The ash beds of the lowermost 0.9 m of the log are massive (facies RCAm) in the basal part and plane parallel laminated (facies CRAh) toward the top (Fig. 13D). In the remaining of the log, the ash is cross-bedded, including the facies RCAt (Fig. 13E) and RCAp (Fig. 13G), or with plane parallel lamination (facies RCAh).

Log 402 (2.4 m of minimum thickness) is from the abandoned channel near its mouth. It is mainly constituted of reworked lapilli interbedded with coarse-grained ash; there are two intercalations of fine-grained ash near the top. Similarly to log 212, the lapilli beds commonly show a vertical transition from massive (facies RLm) to plane parallel lamination (facies RLh). Less commonly, the lapilli beds can be assigned to facies RLs and RLt. Likewise; ash beds show a transition from facies RCAm to facies RCAh. Participation of cross-bedded ash is rare (facies RCAl and RCAt). The fine-grained intercalations are massive or with plane parallel lamination (facies RFAm/h) (Fig. 13I).

Interpretation. In both logs, the presence of reworked pyroclastic beds with massive aspect in the base (facies RLm and RCAm), which show scoured bases and a vertical transition to horizontal lamination (facies RLh and RCAh), is consistent with dilute flows that increased the water–sediment ratio (dilution *sensu* Fisher, 1983). These dilute flows have evolved from type 2 to type 1 by deposition of sediments or addition of water (Smith and Lowe, 1991; Umazano et al., 2008, 2012). The cross-bedded facies indicate the development of straight-crested dunes (facies RCAp), three dimensional dunes (facies RLt and RCAt), plane beds (facies RCAh) and low relief bedforms (facies RCAl). The lapilli beds with crude stratification and inversely-graded pumice fragments (facies RLs) represent hyperconcentrated flows, in which the sediment support mechanisms are buoyancy, grain dispersive forces and turbulence (Smith and Lowe, 1991). The remaining facies RFAm/h, only recorded in log 402, was generated by settling from suspension of pyroclastic fines, probably in ponded zones (Nakayama and Yoshikawa, 1997; Manville et al., 2002; Umazano et al., 2008, 2012). The thin bed of fine-grained ash lying on the pre-2008 soil in the interfluve between the palaeochannel of the Blanco River and the Negro River, probably represents the late stage of flooding before abandonment of the channel.

6.4. Left crevasse splays

Description. These overbank deposits were produced during a few days since May 11, 2008. Here, we only describe the crevasse splay succession located downstream of the Blanco River bridge, which has lobe-shaped cross-section. This crevasse splay flooded the NW–SE oriented airport runway and then flowed through a wetland that is related to the nearby Negro River (Fig. 2B). These deposits are 2.1 m thick near the palaeochannel and thin distally (Fig. 10). Logs 3, 406 and 234 represent successive more distal positions of the splay, whereas log 6 was measured in a low-relief floodplain channel in the wetland (Figs. 4D and 10; see their location in Fig. 2B). Analysis of non channelised zone shows an increase of participation of fine-grained sediment towards distal positions. The more proximal log 3 (1.35 m thick) is characterised by reworked coarse-grained ash interbedded with reworked lapilli. The ash beds show massive aspect (facies RCAm), plane parallel lamination (facies RCAh), ripple-cross lamination (facies RCAr, Fig. 13H) or trough cross-bedding (facies RCAt); a vertical transition from facies RCAm to facies RCAh is ubiquitous (Fig. 13C). The lapilli beds exhibit trough cross-bedding (facies RLt) and, in one level, inversely-graded pumice fragments (facies RLs, Fig. 13B). The logs 406 and 234, both approximately 1.4 m thick, are mostly composed of massive or plane parallel laminated, reworked fine-
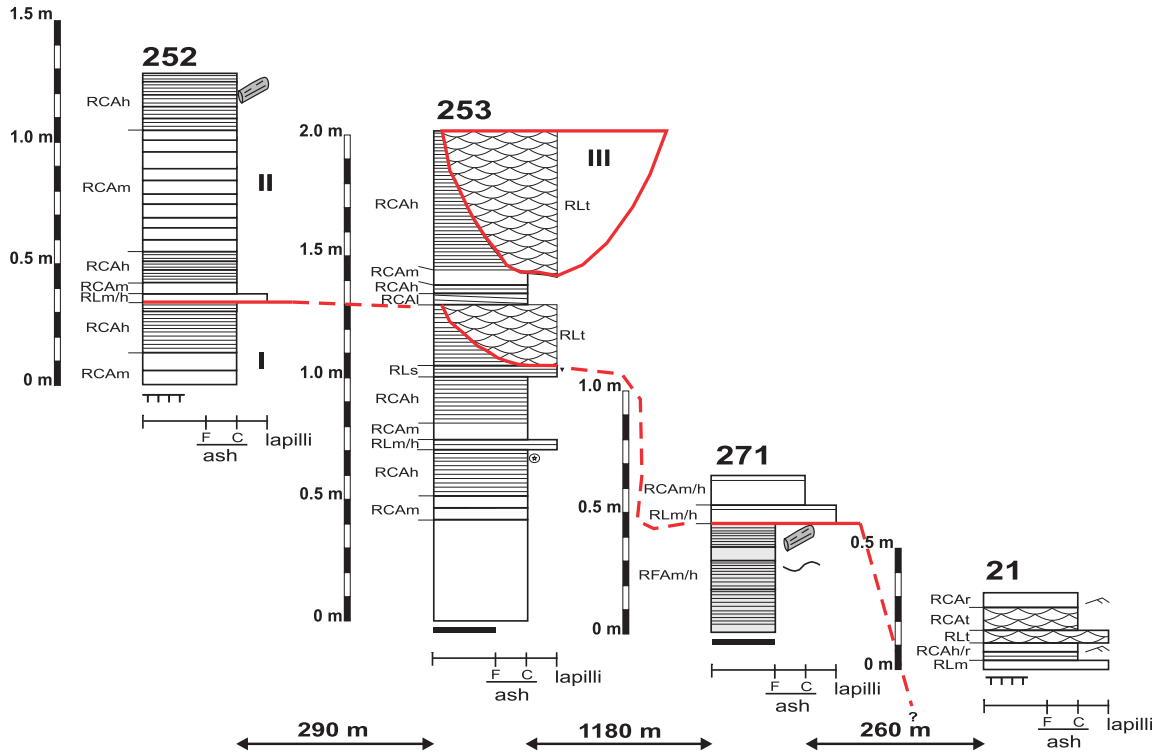
Fig. 8. Detailed sedimentary logs of the channel margin upstream of the logjam zone; they are levelled to the pre-eruptive topography. See location in Fig. 2B.

grained ash (facies RFAm/h). In these logs, the participation of reworked coarse-grained ash (facies RCAm, RCAh and RCAr) and reworked lapilli (facies RLm, RLh and RLs) is reduced and vertical transition from massive facies to laminated facies is very common. The more distal section (log 6) is composed of 0.55 m of massive to plane parallel laminated, reworked fine-grained ash (facies RFAm/h), which is covered by 0.20 m thick and 25 m wide channel deposits constituted of reworked ash (facies RCAt and RCAr) and reworked lapilli (facies RLt).

Interpretation. The succession was mostly generated by dilute flows, including types 1 and 2, and settling from suspension (Smith and Lowe, 1991). The latter process was progressively more common towards distal positions of the floodplain due to ponding of floodwaters. The type 1 dilute flows developed different bedforms including plane beds (facies RCAh and RLh), ripples (facies RCAr) and three-dimensional dunes (facies RCAt and RLt). The type 2 dilute flows formed the massive beds (facies RCAm and RLm). The common vertical transition from massive facies (RCAm and RLm) to laminated facies (RCAh and RLh) indicates a frequent dilution of the flows. The local and subordinate occurrence of facies RLs suggests hyperconcentrated flows (Smith and Lowe, 1991).

6.5. Right crevasse splay

Description. This succession, also originated by overbank floods starting on May 11, 2008, is wedge shaped with a thickness that ranges from 2.2 m along the present channel-margin (logs 252 and 253, Figs. 2B and 11) to about 0.40 m in distal positions of the floodplain (logs 271 and 21, Figs. 2B and 11). Both proximal logs (252 and 253) mostly consist of reworked coarse-grained ash interbedded with reworked lapilli, which are usually arranged in beds with an upward transition from massive facies (RCAm and RLm) to plane parallel laminated facies (RCAh and RLh). Additionally, in log 252 there are two channelised lapilli bodies with trough cross-bedding (facies RLt). In minor amount, stratified lapilli beds with inversely-graded pumice fragments (facies RLs, Fig. 13B) and low angle cross-bedded ash (facies RCAl) were also detected. The log 271 comprises, from bottom to top, massive to plane parallel laminated reworked fine-grained ash (facies RFAm/h), reworked lapilli (facies RLm and RLh) and reworked coarse-grained ash (RCAm and RCAh), successively. The remaining log (21) is an alternation of reworked coarse-grained ash (facies RCAh, RCAr and RCAt) and reworked lapilli (facies RLm and RLt). Reworked coarse ash and lapilli may exhibit centroclinal cross stratification.

Interpretation. Similarly to previously described deposits, the right crevasse-splay was mainly originated by stream currents with different sediment concentration, which covered the continuum between type 1 and type 2 dilute flows (Smith and Lowe, 1991; Umazano et al., 2008, 2012). The latter formed the massive facies (RCAm and RLm), whereas the former originated the cross-bedded and laminated facies from migration of different bedforms (RCAt, RLt, RCAl, RCAr, RCAh and RLh). Locally, deposition from hyperconcentrated flows (facies RLs) and settling from suspension (facies RFAm/h) also occurred.

Fig. 9. Detailed sedimentary logs of filled palaeochannel, and associated delta plain; levelled to the pre-eruptive topography. See location in Fig. 2B and references in Fig. 8.

6.6. Delta plain

Description. Four shallow sedimentary logs were measured to characterise the post May 2008 deposits of this geomorphic setting. Two sections were measured in the sector constructed by

progradation of the terminal lobe of the palaeochannel (logs 275 and 276 in Fig. 9; see locations in Fig. 2B), and two in the area formed by the current course of the river (logs 15 and 282 in Fig. 12; see locations in Fig. 2B). Two lobe-shaped deposits (plan view) were recognised related to the past (palaeochannel) and current

Fig. 10. Detailed sedimentary logs of the left crevasse splay, levelled to the pre-eruptive topography. See location in Fig. 2B and references in Fig. 8.

Fig. 11. Detailed sedimentary logs of the right crevasse splay levelled to the pre-eruptive topography. See location in Fig. 2B and references in Fig. 8.

location of the mouth of the Blanco River. Logs 275 and 15, representing the more proximal part of each depositional lobe, are composed of coarse to fine-grained volcaniclastic sands showing an alternation of beds with massive aspect (facies VSm), cross-bedding (facies VSp and VSl) and plane parallel lamination (facies VSh). Vertical transition from facies VSm to facies VSh is common. The distal logs (276 and 282) are mostly constituted of coarse to fine-grained volcaniclastic sands, which commonly form structureless beds (facies VSm) and, less commonly, show ripple-cross lamination (facies VSr, Fig. 14D), plane parallel lamination (facies VSh) or planar–tabular cross-bedding (facies VSp). In log 282, there is an intercalation of crudely stratified volcaniclastic gravels (facies VGh). In addition, after more than 4 years of the eruption and delivery of abundant material to the sea coast, several low relief ridges were developed on the coast (Fig. 2B). The ridges are located

immediately south of the landing pier and in the northern part of the lobe of the palaeochannel. They are about 1 m high, 10–20 m wide and 0.35–1 km long. In the northernmost area, at least, three ridges were recognised. Similar older ridges were observed along the pre-eruption position of the coastline.

Interpretation. In this geomorphic sector of the study area, deposition occurred from dilute flows with high and low sediment concentration (Smith and Lowe, 1991). Accordingly, the first processes generated the massive beds (facies VSm) and the latter formed diverse bed configurations recorded as different facies (VSp, VSl, VSh, VSr, and VGh). The typical dilution effect (by mixing with water) is inferred from the common occurrence of massive beds that pass upward to plane parallel lamination. The low relief ridges reflect wave reworking of the newly introduced pyroclastic material. In the area located north of the mouth of the Blanco River, successive positions of low relief ridges suggest progradation towards the south-southwest.
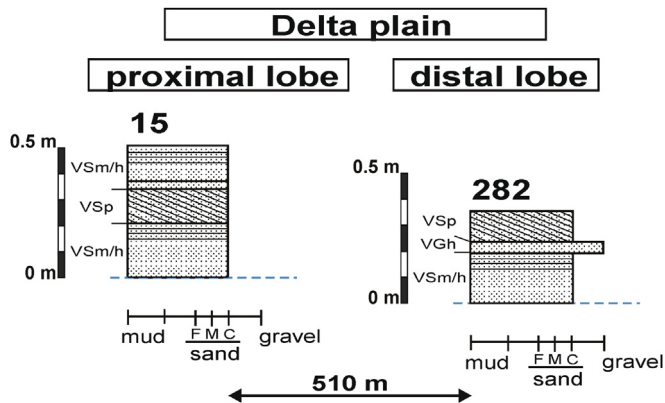
7. Depositional episodes

The sediments of the May 2008 eruption of Chaitén Volcano were divided into four depositional episodes using major (laterally extensive) erosive surfaces. At local scale, each depositional episode is texturally "homogeneous" and, in some cases, the contact between adjacent depositional episodes is related to important changes in sediment composition and grain size (Fig. 16). A single depositional episode can show notorious lateral variations in thickness and grain size (Figs. 9–11). Depositional episodes are named using roman numerals, which indicate the chronological order of deposition in each geomorphic sector. A schematic section showing the spatial and temporal relationships between depositional episodes along the channel-belt is presented in Fig. 17. The deposits of the delta plain are excluded from this analysis because of their reduced thickness and absence of erosive surfaces.

Fig. 12. Detailed sedimentary logs of the delta plain constructed by the actual course of the Blanco River. See location in Fig. 2B and references in Fig. 8.

Table 2
Description and interpretation of facies. Light grey and dark grey backgrounds correspond to reworked pyroclastic and volcaniclastic sediments, respectively.

Facies	Lithology and texture	Sedimentary structures	Interpretation
RLm	Reworked lapilli	Massive, normal grading, low relief scours	Sediment-laden dilute current with high concentration of lapilli
RLh	Reworked lapilli	Plane-parallel lamination, normal grading	Sediment-laden dilute current with low concentration of lapilli, development of plane beds
RLs	Reworked lapilli	Stratification with inverse to normal or inversely-graded pumice fragments	Hyperconcentrated flow
RLt	Reworked lapilli	Trough cross-bedding	Migration of three dimensional dunes composed of lapilli
RCAm	Reworked coarse-grained ash	Massive, normal grading, low relief scours	Sediment-laden dilute current with high concentration of coarse ash
RCAh	Reworked coarse-grained ash	Plane-parallel lamination, normal grading, common deformed laminae	Sediment-laden dilute current with low concentration of coarse ash, development of plane beds
RCAt	Reworked coarse-grained ash	Trough cross-bedding, rare convolute lamination or centroclinal stratification	Migration of three dimensional dunes composed of coarse ash-size, flow around standing trees.
RCAl	Reworked coarse-grained ash	Low-angle cross-bedding	Migration of low relief bedforms composed of coarse ash
RCAp	Reworked coarse-grained ash	Planar-tabular cross-bedding	Migration of two dimensional dunes composed of coarse ash
RCAr	Reworked coarse-grained ash	Ripple-cross lamination, rare convolute lamination	Migration of asymmetrical current ripples composed of coarse ash
RFAm/h	Reworked fine-grained (mud) ash	Massive to plane-parallel lamination, rare convolute deformation	Settling from suspension of pyroclastic fines
VGh	Clast-supported volcaniclastic gravel	Crude horizontal stratification, imbrication	High-energy current flow
VGmm	Matrix-supported volcaniclastic gravel	Massive	Debris flow
VGt	Clast-supported volcaniclastic gravel	Trough cross-bedding	Migration of gravelly three dimensional dunes
VSt	Fine-grained volcaniclastic sand	Trough cross-bedding, occasional centroclinal stratification	Migration of sandy three dimensional dunes, local presence of obstacles (standing trees)
VSl	Coarse-grained volcaniclastic sand	Low-angle cross-bedding	Migration of sandy low relief bedforms
VSm	Coarse-grained volcaniclastic sand	Massive	Dilute flow with high sediment concentration
VSh	Coarse to fine-grained volcaniclastic sand	Plane-parallel lamination	Dilute flow with low sediment concentration, generation of plane beds
VSr	Fine-grained volcaniclastic sand	Ripple-cross lamination	Migration of sandy current ripples
VSp	Coarse-grained volcaniclastic sand	Planar-tabular cross-bedding	Migration of sandy two dimensional dunes

Upstream of the logjam zone, in the margins of the current fluvial course, three depositional episodes were recognised in all sections (I–III in Figs. 8 and 17). The depositional episodes I and II have a relatively uniform metric thickness (range: 1 m–1.8 m), whereas the thickness of the overlying depositional episode III decreases from the boundary of the study area towards the logjam zone from approximately 8 m–1.25 m. Depositional episode I is composed of reworked coarse-grained ash, whereas depositional episode II exhibits similar proportion of volcaniclastic gravels and volcaniclastic sands. Depositional episode III is dominated by volcaniclastic gravels with subordinate amount of volcaniclastic sands, the latter increases its participation towards the logjam zone.

In the filled palaeochannel, three depositional episodes of metric thickness were also recognised (I–III in Figs. 9 and 17). The log located close to the avulsion point shows all depositional episodes, but the more distal log only records the last two. The variation of thickness along the channel axis cannot be sharply detected with the measured logs. In the filled palaeochannel, all depositional episodes are mostly constituted of reworked coarse-grained ash and reworked lapilli.

The succession generated by the left crevasse-splay records four depositional episodes (I–IV in Fig. 10). The first depositional episode is detected in the three more proximal logs (maximum thickness of 0.50 m) and thin out between logs 3 and 234. This depositional episode is composed of reworked tephra and characterised by a decrease in grain size (lapilli and coarse-grained ash to fine-grained ash) towards distal sectors. The second depositional episode, present in all logs, is texturally similar to the first one but the thickness is relatively uniform (range: 0.30 m–0.55 m) in the measured sections. The third depositional episode, characterised by

an alternation of reworked lapilli and reworked coarse-grained ash, also diminishes its thickness from 0.85 m (log 3) towards distal positions (logs 406 and 234) and is eroded by the last depositional episode (IV) in the more distal log. The most recent depositional episode (IV) was only recorded at log 6, has a channel-like geometry and is composed of reworked lapilli and reworked coarse-grained ash; its maximum thickness is 0.25 m and its width reaches approximately 25 m.

Finally, three depositional episodes were observed in the right crevasse-splay (I–III in Fig. 11). Depositional episode I, recorded in the three more proximal logs, probably displays a distal thinning from 1.20 m near the channel-belt to 0 m between logs 271 and 21. The grain size has a similar trend, decreasing from lapilli and coarse-grained ash to fine-grained ash. The following depositional episode II, recognised in all sections, shows a maximum thickness of 0.95 m and wedge out towards distal positions. It is constituted by reworked lapilli and reworked coarse-grained ash. The last depositional episode (III) was only recognised in log 253, where it scours on previous deposits, has channel morphology and is composed of reworked lapilli. Maximum thickness is 0.65 m and maximum width is approximately 50 m.

8. Discussion

The history of the floods, including the trigger mechanisms and relative timing of events, can be inferred from the facies analysis, sequence and features of depositional episodes, and geomorphic evolution. Depositional episodes I–III were controlled by the pre-eruptive topography and proximity to the volcanic edifice (Fig. 17). Accordingly, in the more proximal zone, they are confined
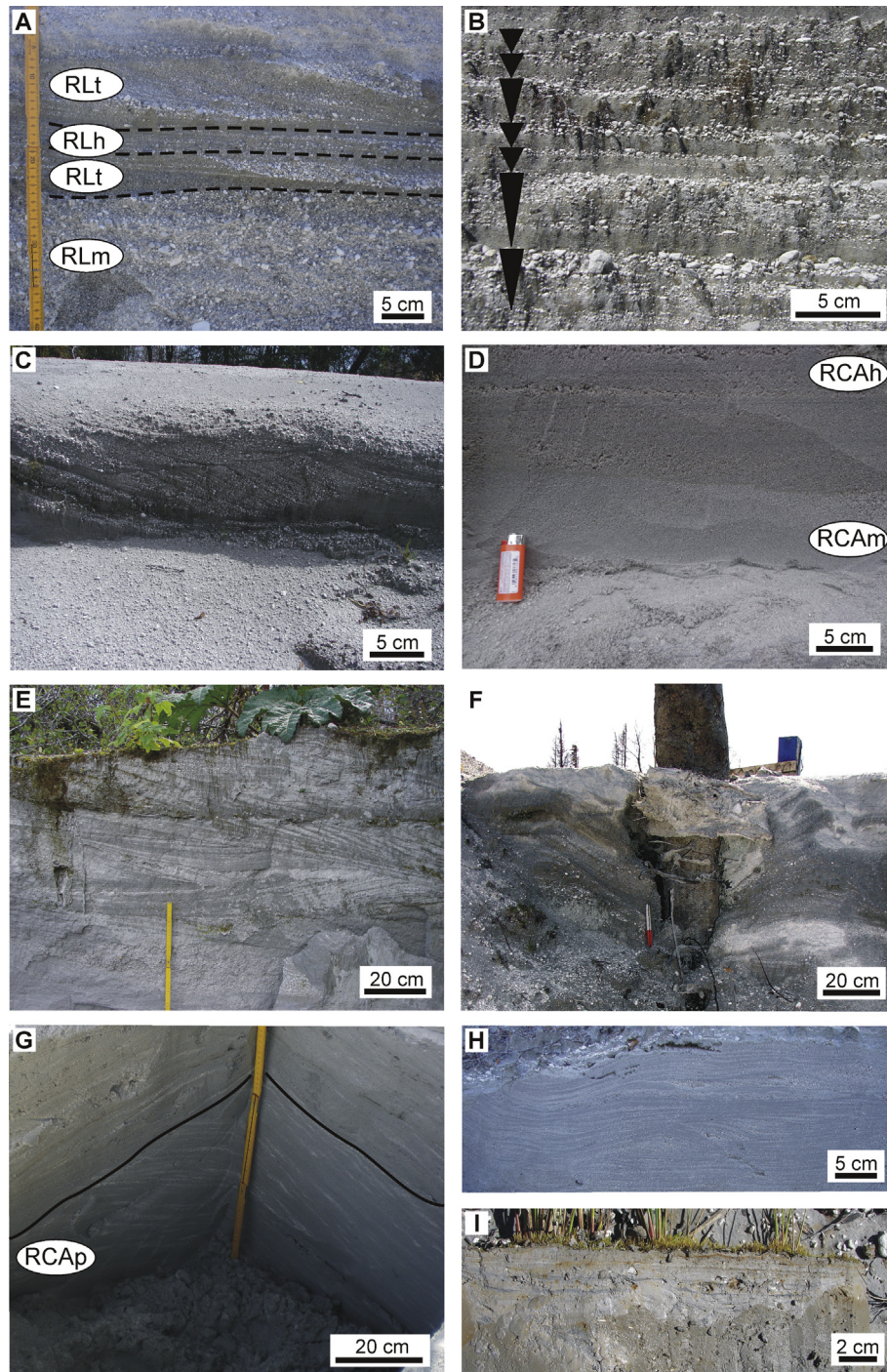
Fig. 13. Examples of reworked pyroclastic facies lacking important participation of epiclastic (older) sediments. (A) Alternation of reworked lapilli with trough cross-bedding (facies RLt) and plane-parallel lamination (facies RLh), which overlie a massive reworked lapilli bed (facies RLm). (B) Stratified reworked lapilli with inversely-graded pumice fragments indicated as vertical triangles (facies RLs). (C) Trough cross-bedded, reworked lapilli (facies RLt). (D) Massive to plane-parallel laminated reworked, coarse-grained ash, facies RCAm and RCAh, respectively. (E) Trough cross-bedded, reworked coarse-grained ash (facies RCAt). (F) Centroclinal stratification in cross-bedded reworked ash. (G) Trench face showing reworked coarse-grained ash with planar-tabular cross-bedding (facies RCAp). (H) Reworked coarse-grained ash with climbing ripples (facies RCAr); (I) Massive to laminated reworked fine-grained ash (facies RFAm/h).

to part of the river valley (Figs. 2B and 7) and show a general reduction of thicknesses from the slopes near the volcanic vent towards the logjam zone (Figs. 8 and 17). In addition, these depositional episodes are thinner and widely distributed in the distal sector of the study area, in particular from 4 km downstream of the logjam zone (Figs. 2B, 7 and 9–11). The first depositional episode, recorded in most geomorphic sectors with similar features

(Figs. 8–11), was probably originated as a response to the high pyroclastic sediment supply and abundant rains in the catchment area (cf. Alfano et al., 2011; Romero, 2011; Pierson et al., 2013). The provenance of detritus in these conditions includes ash-falls and reworked pyroclastic substrates of the 2008 eruption from upland areas. The erosion processes were probably enhanced because of tephra deposits frequently reduce the soil infiltration capacity by
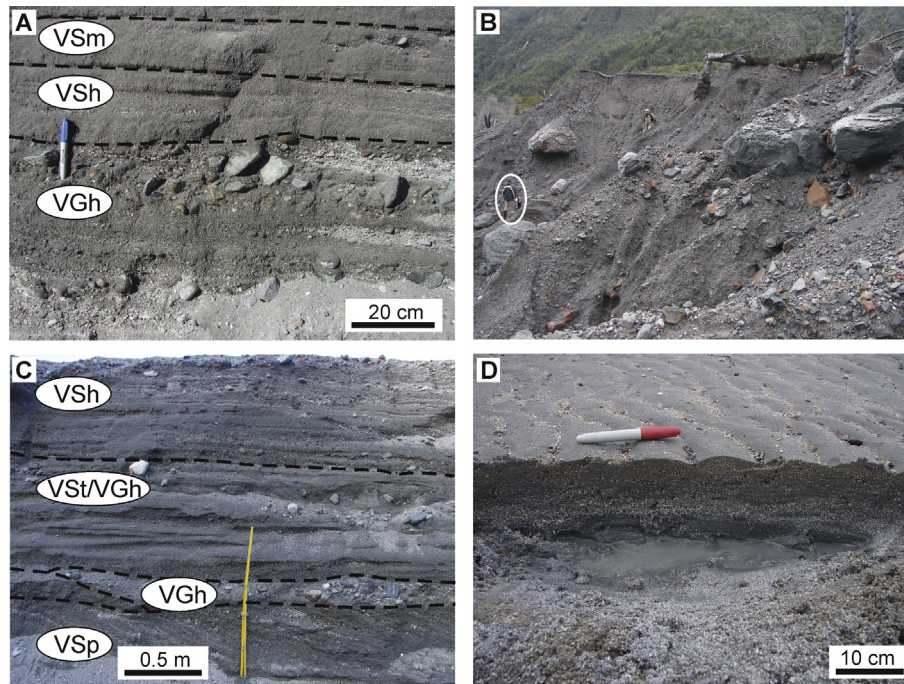
Fig. 14. Examples of volcaniclastic facies. (A) Crudely stratified gravels with some imbricated clasts (facies VGh), which underlie plane-parallel laminated and massive sands (facies VSh and VSm). (B) Massive and matrix-supported gravels (facies VGmm); persons for scale (circled). (C) A complex arrangement of crudely stratified gravels with imbricated clasts (facies VGh) and sands with plane-parallel lamination (facies VSh), trough cross-bedded (facies VSt) or planar–tabular cross-bedded (facies VSp). (D) Wave rippled sands (facies VSr).

developing an impermeable surface crust, which increases the surface runoff from hillslopes to channels (Murata et al., 1966; Waldron, 1967; Leavesley et al., 1989). High sediment influx and/or addition of water increased discharge volume and could have generate overbank flows as those recorded as crevasse-splays. This depositional episode I was mainly characterised by: i) dilute flows along the channel margins upstream of the logjam zone, in the proximal sectors of the crevasse-splays and within the palaeochannel; ii) ponding and settling of suspended sediments in the distal part of the crevasse-splays. In addition, very scarce hyperconcentrated flows were recorded in the right crevasse splay and in the palaeochannel, which suggest a localised and occasional increase of sediment concentration. This depositional event occurred around May 11, 2008 (cf. Pierson et al., 2013).

Depositional episodes II and III are also recorded in most geomorphic sectors, but the records show an important compositional change upstream and downstream of the logjam zone (Figs. 8–11). Upstream of this zone, both depositional episodes are represented by volcaniclastic gravels and volcaniclastic sands, which derived from the mixture of 2008 pyroclastic sediments with older materials. Although the depositional episode II was fully

generated by dilute flows; the overlying depositional episode III shows, from more proximal to more distal positions in relation to the volcanic vent, a transition from *en mase* deposition to grain by grain deposition. This transition can be interpreted as a downstream dilution of debris flows (Smith and Lowe, 1991), a process repeated in several events. Probably the influx of more dilute flows from gullies reduced the sediment concentration and changed the sediment-support mechanisms and resultant facies features (Pierson and Scott, 1985; Rodolfo and Arguden, 1991; Smith and Lowe, 1991; Manville et al., 2009a).

Downstream of the logjam zone the sediments of depositional episodes II and III lack palaeovolcanic materials. The mentioned change in detritus composition is possibly related to the damming of the flow by logs and sediments transported by the Blanco River, a common phenomenon in rivers that cross forests (e.g. Collins and Montgomery, 2002; Wohl, 2011). In this situation, the different floatability of pumice (lapilli and ash) and dense fragments (gravel and sand) generates that older and denser sediments were trapped in the logjam zone and concentrated upstream (Figs. 7 and 8). This phenomenon may occur both when dense flows of pumice-rich juvenile material reached the logjams and overflowed it or during

Fig. 15. Photomosaic of open pit near orthogonal to palaeochannel elongation and close to the margin (location near log 402, Fig. 2B). Note the channel-like geometry of the deposit. White arrows indicate the top of the pre-May 2008 soil and black arrows mark the top of palaeochannel filling.

Fig. 16. Example of contact between sediments of two depositional episodes; in this case the major erosive surface is concave-upward and there is an abrupt increase in grain size; hammer is 25 cm long.

logjam breakage. The dissimilar hydraulic behaviour between these types of sediments have been widely reported (e.g. Smith and Smith, 1985; Manville et al., 1998, 2002).

Presence of deposits of depositional episodes II and III in the filled palaeochannel (Fig. 9), as well as in crevasse-splays from both margins (Figs. 10 and 11), suggests an episodic and widely distributed flooding followed by subsequent avulsion and instauration of the present channel-belt. Accordingly, if the date of avulsion is later than May 20, both depositional episodes occurred from May 11 to May 20. Within the palaeochannel, the flows of depositional episodes II and III were mostly dilute and, subordinately, hyperconcentrated. Settling of suspended sediments also occurred during the third depositional episode near the pre-eruptive shoreline. It suggests flow divergence and ponding of waters in depressed zones between channels.

In the floodplain zone the second depositional episode prograded on pre-eruptive deposits and, on the right margin of the fluvial course, it reached the sea. On the other hand, the depositional episode III prograded on earlier deposits of previous episodes on the left margin and it was erosive and channelised in the right margin. The remaining depositional episode IV, only detected in the left floodplain with channel-like geometry (Fig. 10), represent the last, channelised overbank flow.

Considering the synopsis of the floods, the pyroclastic sediments arrived to the Pacific Ocean mostly via the Blanco River and resulted in a quick progradation of the delta plain. Direct

contribution via ash falls is considered negligible. Progradation is a common phenomenon when sedimentation rate is suddenly increased, and it surpasses the reworking rate by waves and/or tides (Bhattacharya and Walker, 1992; Bhattacharya, 2006). Pyroclastic sediments reached the sea through the pre-eruptive course of the Blanco River until May 15–20 and shifted to the current location of the channel-belt after avulsion. In both situations, the pyroclastic sediments were mixed with older materials by wave and tidal processes.

The availability of a high volume of loose material in the forest and steep slopes of the Blanco River catchment combined with heavy rains were essential for logjam formation. The loose material included both juvenile ash and lapilli; older volcaniclastic sand and gravel; and dead wood. Dead wood mostly resulted from forest devastation by pyroclastic flows (and consequent burning) and mass wasting from the valley slopes. Part of this dead wood is still standing and can be transported in future events. In the Blanco River catchment, still there are several places that contain living and dead standing trees close to the river course that are potential sites for location of future logjams. The location of the logjam zone in a track with increased sinuosity prior to the 2008 eruption and aligned with the mountain front probably suggest a structural (faulting) control. After recovering of the damaged forest near the river course (probably within decades or centuries), the near channel zone will be flanked by large standing trees as occurred previous to the 2008 eruption. In consequence, this process may be typically related to rivers draining forested volcanic highlands. The formation of logjams composed of large logs and gravel is a previously unnoticed and critical factor in hazards evaluation in volcanic forested areas. For the case of the Blanco River catchment, studies of hazard evaluation should include estimation, categorisation and mapping of loose material, and identification and monitoring of river tracks with standing trees near the channel.

9. Conclusions

The 2008 explosive eruption of the Chilean Chaitén Volcano produced abundant loose pyroclastic material that, in combination with abundant rains, steep slopes and large areas of devastated forest, triggered several geomorphic modifications in the adjacent Blanco River. This fluvial system experienced widening of channels, changes in channel design (sinuosity and bar types), damming by logs and sediments, crevassing and channel avulsion, as well as progradation of associated delta plain. All these disturbances occurred in two or three weeks (from May 2 to May 15–20). Most of the geomorphic sectors record three depositional episodes denominated I–III in chronological order. Depositional episode I is
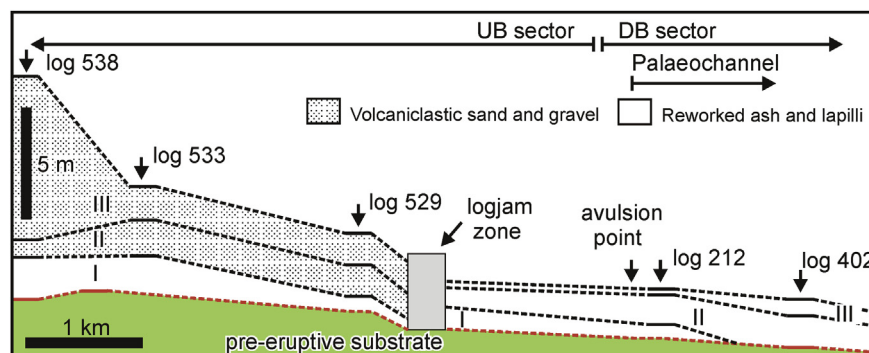

Fig. 17. Schematic representation of depositional episodes (I–III) along the fluvial channel-belt. Note contrasting composition of sediments of depositional episodes upstream and downstream of the logjam zone. See Fig. 2B for location of sections.

composed of reworked (but unmixed) lapilli and ash, which were mainly deposited by dilute flows with different sediment concentration and settling from suspension. Depositional episodes II and III are compositionally heterogeneous: they are constituted by volcaniclastic gravels and sands upstream of the logjam zone; from there to the upper delta plain they are composed of reworked and unmixed tephra; and in the more distal positions (delta plain), they return to be mixed with older epiclastic sediments. Upstream of the logjam zone depositional episodes II and III mostly records debris flows; whereas downstream they were typically originated by dilute flows with different water/sediment ratio and settling from suspension. This important change in composition of detritus and in flow generation is related to the combination of the following factors: i) damming of the flow by logs and sediments and ii) different floatability between pumice (lapilli and ash) and volcaniclastic gravel and sand fragments during logjam's breakage. Logjams played an essential role in the downstream flooding and avulsion of the Blanco River and should be considered in hazards evaluation in volcanic forested regions. Their location is controlled by the presence of standing trees near the channel and also by structural controls.

Acknowledgements

Appendix A. Supplementary data

Supplementary data related to this article can be found at http://dx.doi.org/10.1016/j.jsames.2014.04.007.

References

Alfano, F., Bonadonna, C., Volentik, A.C.M., Connor, C.B., Watt, S.F.L., Pyle, D.M., Connor, L.J., 2011. Tephra stratigraphy and eruptive volume of the May, 2008, Chaitén eruption, Chile. Bull. Volcanol. 73, 613–630.

Bhattacharya, J.P., 2006. Deltas. In: Posamentier, H.W., Walker, R.G. (Eds.), Facies Models Revisited, Society for Sedimentary Geology Special Publication 84, pp. 237–292 (Tulsa).

Bhattacharya, J.P., Walker, R.G., 1992. Deltas. In: Walker, R.G., James, N.P. (Eds.), Facies Models: Response to Sea Level Change. Geological Association of Canada, Tulsa, pp. 157–177.

Bridge, J.S., 1993. Description and interpretation of fluvial deposits: a critical perspective. Sedimentology 40, 801–810.

Carn, S.A., Pallister, J.S., Lara, L., Ewert, J.W., Watt, S., Prata, A.J., Thomas, R.J., Villarosa, G., 2009. The unexpected awakening of Chaitén volcano, Chile. Eos 90, 205–212.

Castro, J.M., Dingwell, D.B., 2009. Rapid ascent of rhyolitic magma at Chaitén volcano, Chile. Nature 461, 780–783.

Collins, B.D., Montgomery, D.R., 2002. Forest development, wood jams and restoration of floodplain rivers in the Puget Lowland, Washington. Restor. Ecol. 10, 237–247.

Cronin, S.J., Neall, V.E., Lecointre, J.A., Palmer, A.S., 1997. Changes in Whangaehu river lahar characteristics during the 1995 eruption sequence, Ruapehu volcano, New Zealand. J. Volcanol. Geotherm. Res. 76, 47–61.

Cronin, S.J., Neall, V.E., Lecointre, J.A., Palmer, A.S., 1999. Dynamic interactions between lahars and stream flow: a case study from Ruapehu volcano, New Zealand. Geol. Soc. Am. Bull. 111, 28–38.

Durant, A.J., Villarosa, G., Rose, W.I., Delmelle, P., Prata, A.J., Viramonte, J.G., 2012. Long-range volcanic ash transport and fallout during the 2008 eruption of Chaitén volcano, Chile. Phys. Chem. Earth A/B/C 45–46, 50–64.

Fisher, R.V., 1983. Flow transformations in sediment gravity flows. Geology 11, 273–274.

Gran, K.B., Montgomery, D.R., 2005. Spatial and temporal patterns in fluvial recovery following volcanic eruptions: channel response to basin-wide sediment loading at mount Pinatubo, Philippines. Geol. Soc. Am. Bull. 117, 195–211.

Gran, K.B., Montgomery, D.R., Halbur, J.C., 2011. Long-term elevated post-eruption sedimentation at mount Pinatubo, Philippines. Geology 39, 367–370.

Graettinger, A.H., Manville, V., Briggs, R.M., 2010. Depositional record of historic lahars in the upper Whangaehu valley, Mt. Ruapehu, New Zealand: implications for trigger mechanisms, flow dynamics and lahar hazards. Bull. Volcanol. 72, 279–296.

Hervé, M., 1976. Estudio geológico de la Falla Liquiñe-Reloncaví en el área de Liquiñe: antecedentes de un movimiento transcurrente (Provincia de Valdivia). In: Congreso Geológico Chileno. No. 1, Actas l: 39. Santiago.

Iroume, A., Andreoli, A., Ulloa, H., Merino, A., da Canal, M., Iroume Jr., A., 2010. Role of large wood (LW) in rivers affected by the 2008 Chaitén volcano explosive eruption. In: AGU Fall Meeting, San Francisco, California, abstract #V21D-2352.

Kataoka, K.S., 2011. Geomorphic and sedimentary evidence of a gigantic outburst flood from Towada caldera after 15 ka Towada-Hachinohe ignimbrite eruption, northeast Japan. Geomorphology 125, 11–26.

Kataoka, K.S., Nakajo, T., 2002. Volcaniclastic resedimentation in distal fluvial basins induced by large-volume explosive volcanism: the Ebisutoge-Fukuda tephra, Plio-Pleistocene boundary, central Japan. Sedimentology 49, 319–334.

Kataoka, K.S., Urabe, A., Manville, V., Kajiyama, A., 2008. Breakout flood from an ignimbrite-dammed valley after the 5 ka Numazawako eruption, northeast Japan. Geol. Soc. Am. Bull. 120, 1233–1247.

Lara, L.E., 2009. The 2008 eruption of the Chaitén Volcano, Chile: a preliminary report. Andean Geol. 36, 125–129.

Lara, L.E., Moreno, R., Amigo, A., Hoblitt, R.P., Pierson, T.C., 2013. The Holocene history of Chaitén volcano: new evidence for a 17th-century eruption. Andean Geol. 40, 249–261.

Leavesley, G.H., Lusby, G.C., Lichty, R.W., 1989. Infiltration and erosion characteristics of selected tephra deposits from the 1980 eruption of Mount St. Helens, Washington, USA. J. Hydrol. 34, 339–353.

Major, J.J., 2003. Post-eruption hydrology and sediment transport in volcanic river systems. Water Resour. Impact 5, 10–15.

Major, J.J., Yamakoshi, T., 2005. Decadal-scale change of infiltration characteristics of a tephra-mantled hillslope at Mount St. Helens, Washington. Hydrol. Process. 19, 3621–3630.

Major, J.J., Mark, L.E., 2006. Peak flow responses to landscape disturbances caused by cataclysmic 1980 eruption of Mount St. Helens, Washington. Geol. Soc. Am. Bull. 118, 938–958.

Major, J.J., Lara, L.E., 2013. Overview of Chaitén volcano, Chile, and its 2008–2009 eruption. Andean Geol. 40, 196–215.

Major, J.J., Pierson, T.C., Dinehart, R.L., Costa, J.E., 2000. Sediment yield following severe volcanic disturbance — a two decade perspective from Mount St. Helens. Geology 28, 819–822.

Major, J.J., Pierson, T.C., Hoblitt, R.P., Moreno, H., 2013. Pyroclastic density currents associated with the 2008–2009 eruption of the Chaitén volcano (Chile): forest disturbances, deposits, and dynamics. Andean Geol. 40, 324–358.

Manville, V., White, J.D.L., Houghton, B.F., Wilson, C.J.N., 1998. The saturation behaviour of Taupo 1800a pumice and some sedimentological implications. Sediment. Geol. 119, 5–16.

Manville, V., Newton, E.H., White, J.D.L., 2005. Fluvial responses to volcanism: resedimentation of the 1800a Taupo ignimbrite in the Rangitaiki River catchment, North Island, New Zealand. Geomorphology 65, 49–70.

Manville, V., Németh, K., Kano, K., 2009a. Source to sink: a review of three decades of progress in the understanding of volcaniclastic processes, deposits, and hazards. Sediment. Geol. 220, 136–161.

Manville, V., Newton, E.H., White, J.D.L., 2009b. Fluvial responses to volcanism: resedimentation of the 1800a Taupo ignimbrite eruption in the Rangitaiki River catchment, North Island, New Zealand. Geomorphology 65, 49–70.

Manville, V., Segschneider, B., Newton, E., White, J.D.L., Houghton, B.F., Wilson, C.J.N., 2009c. Environmental impact of the 1.8 ka Taupo eruption, New Zealand: landscape responses to a large-scale explosive rhyolite eruption. Sediment. Geol. 218, 155–173.

Manville, V., Segschneider, B., White, J.D.L., 2002. Hydrodynamic behavior of Taupo 1800a pumice: implications for the sedimentology of remobilized pyroclasts. Sedimentology 49, 955–976.

Melchor, R.N., Genise, J.F., Sanchez, M.V., Sarzetti, L., Umazano, A.M., 2010. Taphonomy of modern traces in volcaniclastic deposits: the eruption of Chaitén volcano (2008–2010) as a natural laboratory. In: Congreso Latinoamericano de Sedimentología. Abstract Volume: 45. São Leopoldo.

Miall, A.D., 1978. Facies types and vertical profile models in braided river deposits: a summary. In: Miall, A.D. (Ed.), Fluvial Sedimentology. Can. Soc. Pet. Geol. Mem. 5, 597–604. Calgary.

Montgomery, D.R., Panfil, M.S., Hayes, S.K., 1999. Channel-bed mobility response to extreme sediment loading at Mount Pinatubo. Geology 27, 271–274.

Murata, K.J., Dondoli, C., Saenz, R., 1966. The 1963–65 eruption of Irazú volcano, Costa Rica (the period of March 1963 to October 1964). Bull. Volcanol. 29, 765–793.

Nakayama, K., Yoshikawa, S., 1997. Depositional processes of primary to reworked volcaniclastics on an alluvial plain; an example from the Lower Pliocene Ohta tephra bed of the Tokai Group, central Japan. Sediment. Geol. 107, 211–229.

Naranjo, J.L., Stern, C.R., 2004. Holocene tephrochronology of the southernmost part (42°30′–45°S) of the Andean Southern Volcanic Zone. Rev. Geol. Chile 31, 224–240.

Naranjo, J.L., Sigurdsson, H., Carey, S.N., Fritz, W., 1986. Eruption of the Nevado del Ruiz volcano, Colombia, on 13 November 1985: tephra falls and lahars. Science 233, 961–963.

Paruelo, J.M., Beltrán, A., Jobággy, E., Sala, O.E., Golluscio, R.A., 1998. The climate of Patagonia: general patterns and controls on biotic processes. Ecol. Aust. 8, 85–101.

Pierson, T.C., Scott, K.M., 1985. Downstream dilution of a lahar: transition from debris to hyperconcentrated streamflow. Water Resour. Res. 21, 1511–1524.

Pierson, T.C., Major, J.J., Amigo, A., Moreno, H., 2013. Acute sedimentation response to rainfall following the explosive phase of the 2008–2009 eruption of Chaitén volcano, Chile. Bull. Volcanol. 75, 1–17.

Prohaska, F., 1976. The climate of Argentina, Paraguay and Uruguay. In: Schwerdtfeger, W. (Ed.), Climates of Central and South America, World Survey of Climatology 12, pp. 13–112. Amsterdam.

Rodolfo, K.S., Arguden, A.T., 1991. Rain-lahar generation and sediment-delivery systems at Mayon volcano, Philippines. In: Fisher, R.V., Smith, G.A. (Eds.), Sedimentation in Volcanic Settings, Society for Sedimentary Geology Special Publication 45, pp. 71–87. Tulsa.

Romero, J.E., 2011. The evolution of the 2008–2011 eruptive cycle at Chaitén volcano, 42°83′ S, Southern Chile. Pyroclastic Flow. J. Geol. 1, 1–10.

Smith, G.A., Smith, R.D., 1985. Specific gravity characteristics of recent volcaniclastic sediment: implications for sorting and grain size analysis. J. Geol. 93, 619–622.

Smith, G.A., Lowe, D.R., 1991. Lahars: volcano-hydrologic events and deposition in the debris flow-hyperconcentrated flow continuum. In: Fisher, R.V., Smith, G.A. (Eds.), Sedimentation in Volcanic Settings, Society for Sedimentary Geology Special Publication 45, pp. 59–70. Tulsa.

Umazano, A.M., Bellosi, E.S., Visconti, G., Melchor, R.N., 2008. Mechanisms of aggradation in fluvial systems influenced by explosive volcanism: an example from the Late Cretaceous Bajo Barreal Formation, San Jorge basin, Argentina. Sediment. Geol. 203, 213–228.

Umazano, A.M., Bellosi, E.S., Visconti, G., Melchor, R.N., 2012. Detecting allocyclic signals in volcaniclastic fluvial successions: facies, architecture and stacking pattern from the Cretaceous of central Patagonia, Argentina. J. South Am. Earth Sci. 40, 94–115.

Umazano, A.M., Melchor, R.N., Bedatou, E., Bellosi, E.S., Krause, J.M., 2013. Fluvial response to an explosive eruption: the case of the Chaitén volcano and Blanco river (2008, Chile). In: 6th Congreso Latinoamericano de Sedimentología. Actas 1: 49. São Pablo.

Underwood, J.R., Lambert, W., 1974. Centroclinal cross strata, a distinctive sedimentary structure. J. Sediment. Res. 44, 1111–1113.

Vessell, R.K., Davies, D.K., 1981. Non-marine sedimentation in an active fore arc basin. In: Ethridge, F.G., Flores, R.M. (Eds.), Recent and Ancient Nonmarine Depositional Environments: Models for Exploration, Society of Economic Paleontologists and Mineralogists Special Publication 31, pp. 31–45. Tulsa.

Waldron, H.H., 1967. Debris flow and erosion control problems caused by the ash eruptions of Irazu volcano, Costa Rica. U. S. Geol. Survey Bull. 1241-I, 37.

Watt, S.F.L., Pyle, D.M., Mather, T.A., Martin, R.S., Matthews, N.E., 2009. Fallout and distribution of volcanic ash over Argentina following the May 2008 explosive eruption of Chaitén, Chile. J. Geophys. Res. 114, B04207.

Watt, S.F.L., Pyle, D.M., Mather, T.A., 2013. Evidence of mid-to late-Holocene explosive rhyolitic eruptions from Chaitén volcano, Chile. Andean Geol. 40, 216–226.

Wohl, E., 2011. Threshold-induced complex behavior of wood in mountain streams. Geology 39, 587–590.